Neurobiology of Disease

Slow Degradation and Aggregation *In Vitro* of Mutant $GABA_A$ Receptor γ2(Q351X) Subunits Associated with Epilepsy

Jing-Qiong Kang,[1] Wangzhen Shen,[1] Melissa Lee,[1] Martin J. Gallagher,[1] and Robert L. Macdonald[1,2,3]

Departments of [1]Neurology, [2]Molecular Physiology and Biophysics, and [3]Pharmacology, Vanderbilt University Medical Center, Nashville, Tennessee 37212

The $GABA_A$ receptor γ2 subunit nonsense mutation Q351X has been associated with the genetic epilepsy syndrome generalized epilepsy with febrile seizures plus, which includes a spectrum of seizures types from febrile seizures to Dravet syndrome. Although most genetic epilepsy syndromes are mild and remit with age, Dravet syndrome has a more severe clinical course with refractory seizures associated with developmental delay and cognitive impairment. The basis for the broad spectrum of seizure phenotypes is uncertain. We demonstrated previously that the $GABA_A$ receptor γ2 subunit gene Q351X mutation suppressed biogenesis of wild-type partnering α1 and β2 subunits in addition to its loss of function. Here we show that γ2S(Q351X) subunits have an additional impairment of biogenesis. Mutant γ2(Q351X) subunits were degraded more slowly than wild-type γ2 subunits and formed SDS-resistant, high-molecular-mass complexes or aggregates in multiple cell types, including neurons. The half-life of γ2S(Q351X) subunits was ~4 h, whereas that of γ2S subunits was ~2 h. Mutant subunits formed complexes rapidly after synthesis onset. Using multiple truncated subunits, we demonstrated that aggregate formation was a general phenomenon for truncated γ2S subunits and that their Cys-loop cysteines were involved in aggregate formation. Protein aggregation is a hallmark of neurodegenerative diseases, but the effects of the mutant γ2S(Q351X) subunit aggregates on neuronal function and survival are unclear. Additional validation of the mutant subunit aggregation *in vivo* and determination of the involved signaling pathways will help reveal the pathological effects of these mutant subunit aggregates in the pathogenesis of genetic epilepsy syndromes.

Introduction

The genetic epilepsy syndrome generalized epilepsy with febrile seizures plus (GEFS+) occurs in families with members who have a spectrum of epilepsy phenotypes, including febrile seizures, febrile seizures plus, myoclonic-astatic epilepsy, and Dravet syndrome (Scheffer and Berkovic, 1997; Scheffer et al., 2001), and has been associated mostly with missense mutations in *SCN1A* (sodium channel, voltage-gated, type I, α subunit) and *GABRG2* ($GABA_A$ receptor γ2 subunit gene). Dravet syndrome is a severe epilepsy syndrome that is characterized by febrile and afebrile seizures, generalized, focal, and myoclonic seizures, developmental delay, and cognitive impairment. The pathophysiological basis for GEFS+ and for the broad spectrum of seizure phenotypes is uncertain. Dravet syndrome has been associated mostly with SCN1A (Berkovic et al., 2006; Ohmori et al., 2006) and also with GABRG2 nonsense mutations (Harkin et al., 2002; Hirose, 2006). We recently reported that mutant truncated γ2S(Q351X) gene subunits were trafficking deficient, accumulated intracellularly, and suppressed biogenesis of wild-type γ2S and partnering α and β subunits by oligomerizing with them (Kang et al., 2009b), thus reducing cell-surface $GABA_A$ receptors to levels lower than produced by loss of one GABRG2 allele (Crestani et al., 1999; Kang et al., 2009b). In that study, we used the γ2S subunit, the major γ2 subunit splicing isoform, and unexpectedly observed that mutant γ2S(Q351X) subunits formed SDS-resistant, high-molecular-mass protein complexes when transfected into multiple cell lines and cultured rat neurons. The cellular consequences of γ2S(Q351X) subunit complexes, however, are uncertain. Most pedigrees associated with $GABA_A$ receptor subunit mutations express relatively benign epilepsy phenotypes, such as simple febrile seizures and childhood absence epilepsy (Kang and Macdonald, 2009). However, some individuals with GABRG2 (Harkin et al., 2002; Hirose, 2006), SCN1A (Berkovic et al., 2006), or SCN2A (Kamiya et al., 2004; Shi et al., 2009) mutations, especially truncation or exonic deletion mutations, manifest the severe Dravet syndrome and develop encephalopathy after prolonged high temperature or after vaccination (Berkovic et al., 2006). It is unclear also why some individuals in families with genetic epilepsy syndromes develop mesial temporal sclerosis (Cohen-Gadol et al., 2005; Xu et al., 2007). The extended clinical spectrum in addition to seizures suggests that additional unidentified pathological events, such as abnormal cellular signaling or cellular dysfunction (Li et al., 2000), may occur in these patients.

Received May 6, 2010; revised July 29, 2010; accepted Aug. 4, 2010.

This work was supported by a research grant from Citizens United for Research in Epilepsy (J.-Q.K.) and National Institutes of Health Grants K02 NS 055979 (M.J.G.) and R01 NS51590 (R.L.M.). We thank Joan Skluzacek, president of IDEALeague for Dravet Syndrome, for encouragement to J.-Q.K. to pursue the study.

Correspondence should be addressed to Dr. Jing-Qiong Kang, Vanderbilt University Medical Center, 6140 Medical Research Building III, 465 21st Avenue South, Nashville, TN 37232-8552. E-mail: jingqiong.kang@vanderbilt.edu.

DOI:10.1523/JNEUROSCI.2320-10.2010

 0270-6474/10/3013895-11$15.00/0

In this study, we demonstrated that truncated γ2S subunits were more prone to form protein complexes than wild-type γ2S subunits when expressed alone or with subunit assembly partners. We also found that mutant γ2S(Q351X) subunits formed these complexes rapidly after onset of subunit translation but were degraded inefficiently. Both proteasomal and lysosomal inhibition slowed degradation of the mutant subunits, and their presence increased conjugation of polyubiquitin chains. Perturbation of the ubiquitin–proteasome pathway occurs at onset of many degenerative diseases (Berke and Paulson, 2003), and the present study implies that at least some trafficking-deficient epilepsy mutations may engage signaling pathways that are shared with many other defective mutant proteins. However, it is unclear whether and how the trafficking-deficient, but stable, mutant γ2(Q351X) subunits and the high-molecular-mass protein complexes contribute to epileptogenesis. It will require future study to determine whether these protein complexes contribute to shaping the disease phenotype *in vivo*.

Materials and Methods

Expression vectors with $GABA_A$ receptor subunits. The cDNAs encoding human $GABA_A$ receptor subunits α1, β2, and γ2Ss were constructed as described previously (Kang and Macdonald, 2004). Yellow fluorescent protein (YFP)-tagged $GABA_A$ receptor γ2S subunits were as described previously (Kang and Macdonald, 2004). The FLAG (DYKDDDDK) epitope was inserted between amino acids 4 and 5 in the N terminus of the mature protein (Kang et al., 2009b). All mutations were generated using the QuikChange site-directed mutagenesis kit (Stratagene) and confirmed by DNA sequencing in the Vanderbilt DNA Core.

Cell culture and transfection. HEK 293T, COS-7, and HeLa cells were replenished with DMEM supplemented with 10% FBS and antibiotics. Rat cortical and hippocampal neurons were prepared as before (Kang et al., 2009a,b) and were transfected using the Ca^{2+}-phosphate method. COS-7 cells were transfected with using the Ca^{2+}-phosphate method. HEK 293T and HeLa cells were cotransfected with 1–3 μg of each subunit for each 60 mm^2 dish in the receptor condition or 3 μg in the single subunit condition with Fugene, and the total cell lysates were prepared 48 h later. Neurons were transfected with 15 μg of cDNA at day 7 in culture and were harvested 8 d after transfection. Four 100 mm^2 dishes of neurons were transfected of each subunit in each experiment to ensure enough proteins for immunoblotting assay attributable to low transfection efficiency in neurons.

[^{35}S] radiolabeling metabolic pulse-chase assays. The pulse-chase assays for both γ2 subunit alone or γ2 subunit with α1 and β2 subunits were modified from our previously published protocol (Gallagher et al., 2007; Kang et al., 2009a,b). Briefly, forty-eight hours after transfection, the cells were placed in starving medium that lacked methionine and cysteine (Invitrogen) and incubated at 37°C for 30 min. The starving medium was then replaced by 1.5 ml of [^{35}S] radionuclide methionine [100–250 μCi/ml (1 Ci = 37GBq); PerkinElmer Life and Analytical Sciences] labeling medium for 20 min at 37°C. The labeling medium was then changed to chase medium for a series of different time points. FLAG-tagged $GABA_A$ receptor subunits were then immunoprecipitated from radiolabeled lysates with anti-FLAG M2-agarose affinity gel by rotating at 4°C overnight. The immunoprecipitated products were eluted from the beads with FLAG peptide (Sigma-Aldrich). The immunopurified subunits were then analyzed by 12.5% SDS-PAGE and exposed on a digital PhosphorImager (GE Healthcare).

Measurement of total $\gamma 2S^{HA}$ subunit expression using flow cytometry. Measurement of total expression of $GABA_A$ receptor subunits using flow cytometry has been described previously (Lo et al., 2008). Briefly, transfected HEK 293T cells were removed from the dishes by trypsinization and then resuspended in FACS buffer (PBS, PBS supplemented with 2% FBS, and 0.05% sodium azide). After washes with FACS buffer and permeabilization with Cytofix/cytoperm (BD Biosciences) for 15 min, cells were incubated with anti-hemagglutinin (HA) antibody directly conjugated with fluorophore Alexa Fluor-647 (1:200) for 1 h at 0°C. Cells were then washed with FACS buffer and fixed with 2% paraformaldehyde. The acquired data were analyzed using FlowJo 7.1 (Treestar).

Live-cell confocal microscopy and fluorescence quantification. Live-cell confocal microscopy in HEK 293T cells, COS-7 cells, and hippocampal neurons was performed as reported previously (Kang and Macdonald, 2004). Briefly, live cells were directly imaged using an inverted Carl Zeiss laser scanning microscope (model 510) with a 63×, 1.4 numerical aperture or 40×, 1.3 numerical aperture oil-immersion lens, 2–2.5× zoom. COS-7 cells and hippocampal neurons were plated on poly-D-lysine-coated, glass-bottom imaging dishes at the density of 0.5–1 × 10^5 cells. The total fluorescence intensity of the cell body or the somata area and the processes including both axons and dendrites in the neurons were measured using MetaMorph imaging software by specifically defining the region of interest.

Immunoprecipitation and Western blot analysis. For immunoprecipitation, wild-type $\gamma 2S^{FLAG}$ and $\gamma 2S(Q351X)^{FLAG}$ subunits were purified by incubating cell lysates (1–1.5 mg) overnight with 50 μl of agarose-immobilized anti-FLAG M2 antibody (Sigma-Aldrich). The antibody resin was pelleted by centrifugation and washed three times with lysis buffer. FLAG-tagged subunits were liberated by incubation with FLAG peptide (Sigma-Aldrich) for 30 min on ice. For total protein SDS-PAGE, 50–80 μg of cell lysates per lane was loaded. Rabbit polyclonal anti-FLAG or anti-$GABA_A$ receptor γ2 subunit antibody was purchased from Sigma or Alomone Labs. A mouse monoclonal antibody (clone p4G7) directed against monoubiquitin and polyubiquitin was purchased from Covance Research Products.

Data analysis. Proteins were quantified by ChemiImager AlphaEaseFC software, and data were normalized to either wild-type subunits or loading controls. Both the lower- and higher-molecular-mass bands were included for the quantification in all experiments except otherwise specified. The integrated density volumes (IDVs) of the wild-type subunits were arbitrarily taken as 1. The total IDVs of the mutant subunits were then normalized to the wild-type subunits. Data from pulse-chase experiments were quantified using Quantity One software (Bio-Rad). Numerical data were expressed as mean ± SEM. When wild-type data were arbitrarily taken as 1, column statistics were used. Statistical significance using Student's unpaired *t* test (Prism; GraphPad Software) was taken as $p < 0.05$.

Results

Mutant γ2S(Q351X) subunits accumulated, aggregated, and formed high-molecular-mass protein complexes in both HEK 293T cells and rat cortical neurons

Several γ2 subunit missense mutations have been associated with genetic epilepsy syndromes, including the γ2 subunit mutation R43Q, which is associated with childhood absence epilepsy and febrile seizures (Wallace et al., 2001), and the γ2 subunit mutation K289M, which is associated with GEFS+ (Baulac et al., 2001) (Fig. 1*A*, left). Several γ2 subunit nonsense mutations have been associated also with genetic epilepsy syndromes, including the γ2 subunit nonsense mutation Q351X, which is associated with GEFS+ and Dravet syndrome, and the premature translation-termination codon (PTC) is located in the transmembrane domain 3 (TM3)–TM4 loop (Fig. 1*A*, right). We have shown that the PTC results in loss of the C-terminal 78 aa and produces a stable, truncated subunit that is retained in the endoplasmic reticulum (ER) (Kang et al., 2009b). When coexpressed with α1 and β2 subunits and immunoblotted with an anti-human γ2 subunit antibody, wild-type γ2S and mutant γ2S(R43Q) and γ2S(K289M) subunits all migrated at the same molecular mass, predicted to be ~50 kDa (Fig. 1*B*, band 4; U). The truncated mutant γ2S(Q351X) subunit migrated at a lower molecular mass predicted to be ~40 kDa (Fig. 1*B*, band 5; U, red arrow) but unexpectedly also formed a protein complex that migrated at a high molecular mass (~80–100 kDa) (Fig. 1*B*, band 1; U). After digestion with *N*-glycosidase F (PNGase F), a glycosidase that

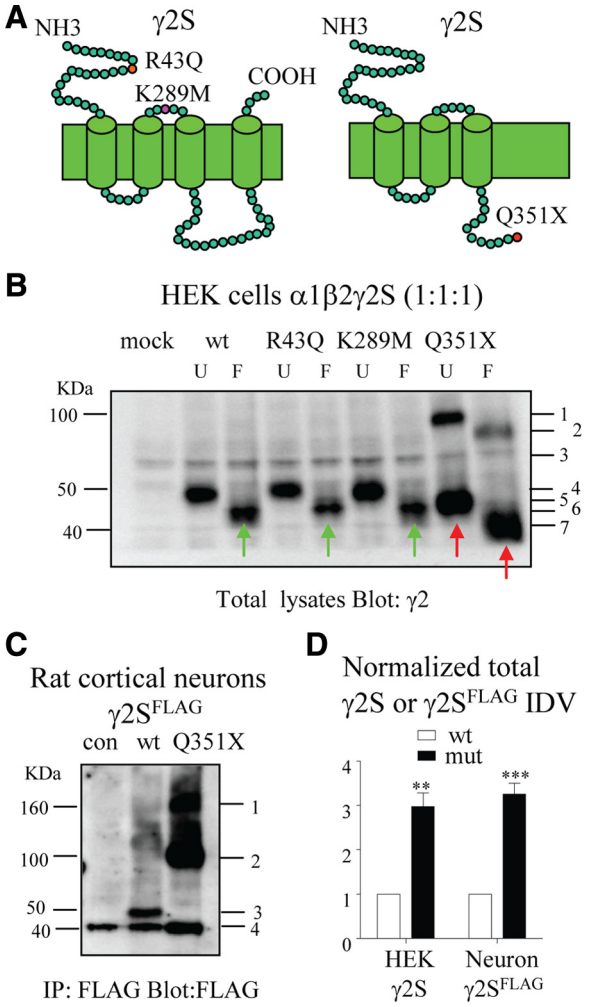

Figure 1. Mutant γ2S(Q351X) subunits self aggregated and formed high-molecular-mass protein complexes. ***A***, Schematic topologies of wild-type and mutant γ2S subunits are presented. The red dots represent the locations of the γ2S subunit mutations R43Q, K289M, and Q351X. ***B***, Total lysates (30 μg) from cells mock transfected with "empty" plasmids (mock) or with wild-type (wt) or mutant α1β2γ2S subunits were analyzed by immunoblot using a polyclonal rabbit anti-γ2 subunit antibody. Bands 1 and 2 are the PNGase F untreated (U, band 1) or treated (F, band 2) high-molecular-mass protein complexes. Band 3 is a nonspecific band detected with the polyclonal rabbit anti-γ2 subunit antibody. Bands 4 and 6 are PNGase F untreated (U, band 4) or treated (F, band 6, green arrows) monomeric wild-type γ2S and mutant γ2S(R43Q) or γ2S(K289M) subunits. Bands 5 and 7 are PNGase F untreated (U, band 5, red arrow) or treated (F, band 7) monomeric mutant γ2S(Q351X) subunits. ***C***, Rat cortical neurons untransfected (con) or transfected with $\gamma2S^{FLAG}$ (wt) or $\gamma2S(Q351X)^{FLAG}$ (Q351X) subunits were lysed, immunopurified with anti-FLAG antibody, and analyzed by SDS-PAGE with anti-FLAG antibody. Bands 1 and 2 are the high-molecular-mass protein complexes that migrated at ~160 kDa (band 1) and ~80 kDa (band 2). Band 3 is the monomeric wild-type $\gamma2S^{FLAG}$ subunit, and band 4 is a nonspecific band that overlapped the monomeric mutant $\gamma2S(Q351X)^{FLAG}$ subunits. ***D***, The total IDVs of both γ2S or γ2S(Q351X) subunits in HEK 293T cells (HEK) or $\gamma2S^{FLAG}$ or $\gamma2S(Q351X)^{FLAG}$ subunits in neurons (Neuron) were measured by subtracting the control band or the equivalent area if there was no distinct band. Both the lower- and higher-molecular-mass bands were included. The IDVs of the wild-type subunits were then taken as 1. The total IDVs of the mutant subunits were then normalized to the wild-type subunits ($n = 4$ for both HEK and Neuron; $^{**}p < 0.01$; $^{***}p < 0.001$ vs wild type).

removes all N-linked carbohydrates attached in either ER or trans-Golgi regions, wild-type γ2S and mutant γ2S(R43Q), γ2S(K289M), and γ2S(Q351X) subunits were all shifted to lower molecular masses (Fig. 1*B*, band 6 green arrows and band 7 red arrow; F) as predicted by their glycosylation patterns. In addition, the high-molecular-mass protein complex was shifted also to a

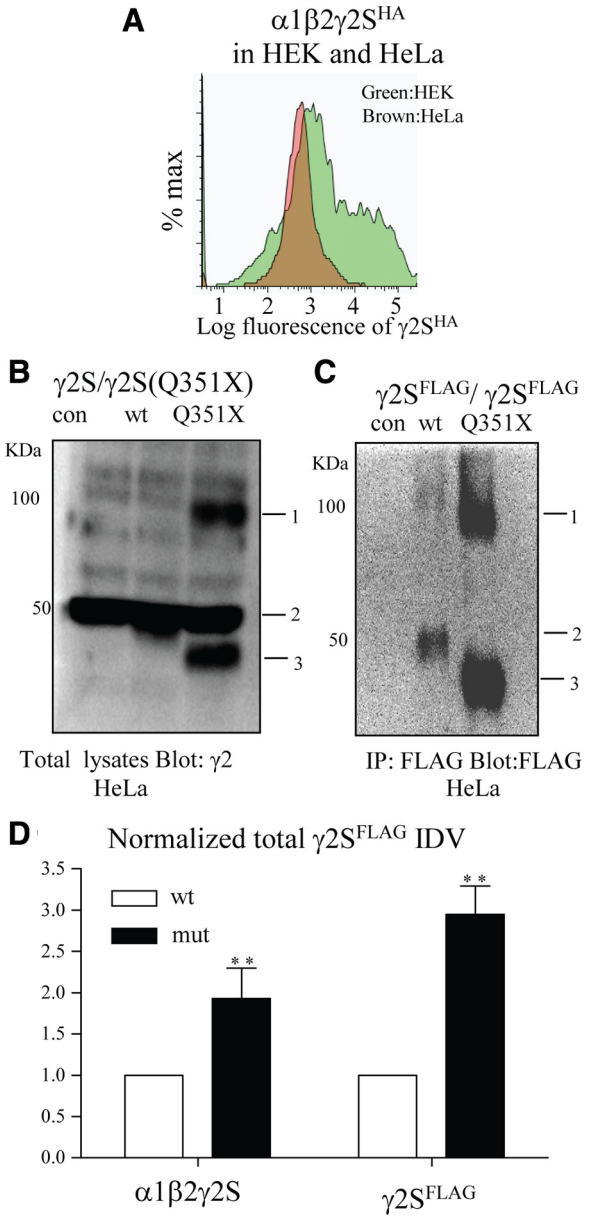

Figure 2. γ2S(Q351X) subunit protein aggregated and formed high-molecular-mass protein complexes in HeLa cells, which have low subunit expression. ***A***, The flow cytometry histograms depict the total expression levels of $\gamma2S^{HA}$ subunits in either HEK 293T (green) or HeLa (brown) cells transfected with the same amounts of cDNAs as detected with fluorescently conjugated anti-human HA antibody (HA–Alexa Fluor-647). The total expression of $\gamma2S^{HA}$ subunits in HeLa cells was normalized to the $\gamma2S^{HA}$ in HEK 293T cells. ***B***, ***C***, HeLa cells were transfected with wild-type α1β2γ2S or mutant α1β2γ2S(Q351X) subunits (***B***) or with $\gamma2S^{FLAG}$ or $\gamma2S(Q351X)^{FLAG}$ subunits alone (***C***). At 48 h after transfection, the cells were lysed, and subunits in the lysates were either detected directly by SDS-PAGE (80 μg/lane) or were immunopurified with FLAG beads and then analyzed by SDS-PAGE using 1.5 mg of protein lysate per sample. In both ***B*** and ***C***, band 1 is the high-molecular-mass protein complex that migrated at ~160 kDa, and band 3 is the monomeric mutant $\gamma2S(Q351X)^{FLAG}$ subunit. In ***B***, band 2 is a nonspecific band that overlapped the monomeric wild-type γ2S subunits, and in ***C***, band 2 is the monomeric wild-type $\gamma2S^{FLAG}$ subunit. ***D***, The total IDVs of $\gamma2S^{FLAG}$ or $\gamma2S(Q351X)^{FLAG}$ subunits when coexpressed with α1 and β2 subunits (left) or when expressed alone (right) in HeLa cells were measured by subtracting the control band or the equivalent area if there was no distinct band. Both lower- and higher-molecular-mass bands were included. The IDVs of wild-type subunits were then taken as 1. Expression of total wild-type protein was also taken as 1. The total IDVs of the mutant subunits were then normalized to the wild-type subunits ($n = 4$ for both ***B*** and ***C***, $^{**}p < 0.01$ vs wild type). con, Control; mut, Mutant; wt, wild type.

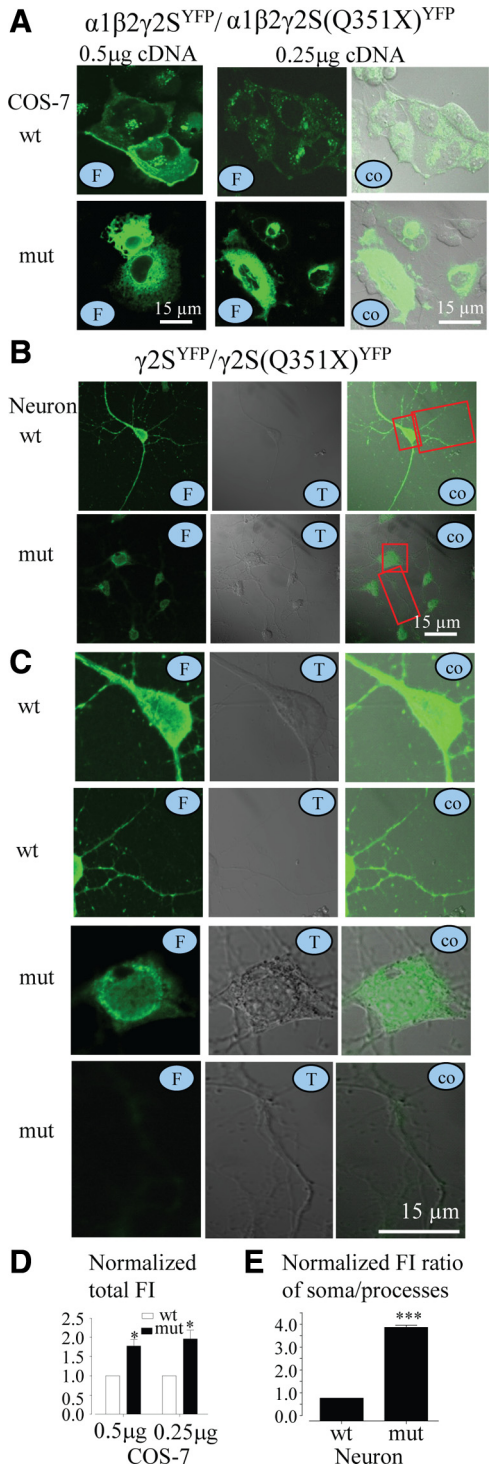

Figure 3. γ2S(Q351X)^{YFP} subunit protein accumulated intracellularly in live cells. ***A***, COS-7 cells were cotransfected with α1 and β2 subunits and wild-type γ2S^{YFP} (wt) or mutant γ2S(Q351X)^{YFP} (mut) subunits using the calcium phosphate precipitation method with different amounts of subunit cDNAs. Images were acquired 2 d after transfection. ***B***, ***C***, Cultured rat hippocampal neurons were cotransfected with wild-type γ2S^{YFP} or mutant γ2S(Q351X)^{YFP} subunits and were imaged using confocal microscopy 8 d after transfection. ***C***, Enlarged views of wild-type and mutant receptors in neuronal somata and processes are shown in boxed areas in ***B***. T, Transmitted image; wt, wild-type γ2S^{YFP} subunits; mut, mutant γ2S(Q351X)^{YFP} subunits; co, colocalized images; F, fluorescent images. ***D***, ***E***, The total fluorescence intensities of cells were measured using the MetaMorph imaging software. In ***D***, the total fluorescence from cells expressing wild-type γ2S^{YFP} subunit-containing receptors (wt) was arbitrarily taken as 1, and the total fluorescence from cells expressing mutant γ2S(Q351X)^{YFP} subunit-containing receptors (mut) was normalized to wild-type levels. In ***E***, the total fluorescence of both neuronal somata and processes (including both axon and dendrites) were measured, and the fluorescence intensity ratios of the areas of the somata over processes were quantified. The fluorescence intensity (FI) ratios of wild-type subunits were arbitrarily taken as 1, and the fluorescence intensity ratios of mutant subunits were normalized to wild-type levels ($n = 14–15$ for COS-7 and $n = 11$ for neurons from four different transfections; $^{*}p < 0.05$, $^{***}p < 0.001$ vs wt).

lower molecular mass by PNGase F digestion (Fig. 1*B*, band 2; F), suggesting that the protein complex contained glycoproteins including γ2S subunits as detected by the anti-γ2 antibody.

A similar high-molecular-mass complex was also formed in cultured rat cortical neurons (Fig. 1*C*) (for an enlarged view, see supplemental Fig. 1, available at www.jneurosci.org as supplemental material). In neurons 8 d after transfection with either wild-type γ2S^{FLAG} or mutant γ2S(Q351X)^{FLAG} subunits, immunopurification of the total cell lysates with FLAG-conjugated beads and blotting with anti-FLAG antibody after SDS-PAGE revealed that wild-type subunits showed only a single distinct band at the predicted mass of a γ2S^{FLAG} subunit (Fig. 1*C*, band 3; wt). In contrast, mutant subunits formed substantial amounts of high-molecular-mass protein complex at ~80 kDa (Fig. 1*C*, band 2; Q351X) and ~160 kDa (Fig. 1*C*, band 1; Q351X) in addition to a distinct band at the predicted mass of a γ2S(Q351X)^{FLAG} subunit (Fig. 1*C*, band 4; Q351X), which overlapped the nonspecific band seen in untransfected neurons (Fig. 1*C*, band 4; con). Interestingly, the protein complex that migrated at ~160 kDa was more prominent in neurons than in HEK 293T cells, suggesting that longer time after transfection may favor formation of the high-molecular-mass protein complex. When normalized to the total wild-type subunit protein, the mutant subunit protein increased approximately threefold (2.98 ± 0.45 for HEK cells, $n = 4$; 3.27 ± 0.32 for neurons, $n = 4$), suggesting that mutant subunits were more stable than wild-type subunits (Fig. 1*D*).

Mutant γ2S(Q351X) subunits also aggregated in HeLa cells, which have much lower subunit expression

Formation of the mutant γ2S(Q351X) subunit high-molecular-mass protein complexes could have been attributable only to subunit overexpression. If so, reducing the protein expression level should reduce or eliminate the complexes. HeLa cells are frequently used for studying nonsense-mediated mRNA attributable to their low transfection efficiency and low levels of protein expression (Linde et al., 2007; Kang et al., 2009a). Therefore, we first determined the relative expression levels of wild-type γ2S subunits when coexpressed with α1 and β2 subunits in HeLa cells with the same amounts of cDNA used for HEK 293T cell transfections and measured subunit expression levels using the quantitative method of flow cytometry to compare subunit expression levels in each cell type (Fig. 2*A*). Consistent with previous studies, $GABA_A$ receptor subunit expression levels were much lower in HeLa cells than in HEK 293T cells, although the total number of cells transfected was not significantly different. For example, using the quantitative technique flow cytometry, 45–60% of HeLa and 50–65% of HEK cells had positive fluorescent signals. With the γ2S^{HA} levels in HEK 293T cells arbitrarily taken as 100%, the expression level of γ2S^{HA} subunits in HeLa cells was only 16.7% of that in HEK 293T cells ($n = 6$ from four different transfections). We then used Western blotting to determine whether the high-molecular-mass protein complex formed in HeLa cells. When either untagged γ2S subunits were coexpressed with α1 and β2 subunits or tagged γ2S^{FLAG} subunits were expressed alone (Fig. 2*B*,*C*), both mutant γ2S(Q351X) and

←

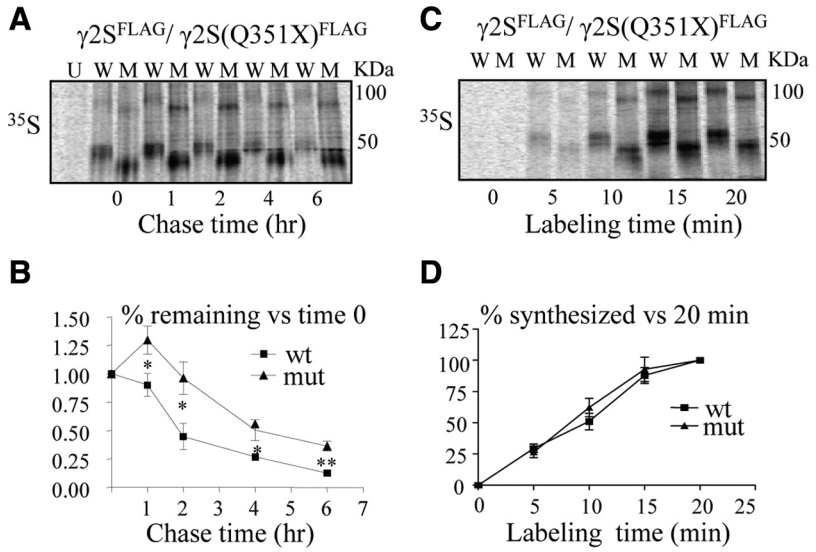

Figure 4. Mutant γ2S(Q351X) subunits formed dimers rapidly and were degraded slowly. ***A–D***, [^{35}S] pulse-labeled untransfected cells (U) or cells transfected with γ2S^{FLAG} (W) or γ2S(Q351X)^{FLAG} (M) subunits were lysed, immunopurified using anti-FLAG antibody, and analyzed by SDS-PAGE. ***A***, ***B***, After 20 min of labeling, cells were chased for the indicated times (***A***). The percentage radioactivity relative to the amounts of radioactivity measured at time 0 for the 100 and 50 kDa bands at each chase time were plotted for either wild-type or mutant subunits (***B***) (*$p < 0.05$, **$p < 0.01$ vs wild type; $n = 5$). ***C***, ***D***, Cells expressing γ2S^{FLAG} or γ2S(Q351X)^{FLAG} subunits were pulse labeled for the indicated times and lysed for immunopurification and SDS-PAGE (***C***). The percentage radioactivity incorporated during subunit synthesis for the 100 and 50 kDa bands at each labeling time was plotted by normalizing to the value obtained at 20 min for either wild-type or mutant subunits (***D***) ($n = 4$). Mut, Mutant; wt, wild type.

γ2S(Q351X)^{FLAG} subunits formed substantial high-molecular-mass complexes that were resistant to SDS. In both cases, the total amounts of mutant subunits were higher than wild-type subunits. Relative to wild-type subunit levels, the total amount of the mutant subunit protein was 1.93 ± 0.37 times higher for γ2S(Q351X) subunits when cotransfected with α1 and β2 subunits and was 2.95 ± 0.34 times higher for γ2S(Q351X)^{FLAG} subunit protein when transfected alone (Fig. 2*D*). Given that similar amounts of HeLa and HEK 293T cells were transfected but that much less total protein was expressed in HeLa cells, it is unlikely that the formation of the mutant subunit aggregates in HeLa cells was attributable only to overexpression.

Mutant γ2S(Q351X) subunits accumulated intracellularly in both live non-neuronal cells and rat hippocampal neurons

Because the total amount of mutant γ2S(Q351X) subunits was higher than wild-type subunits in whole-cell lysates, we then extended the study to determine the cellular location of mutant subunits in live cells using confocal microscopy. YFP-tagged human γ2S^{YFP} and γ2S(Q351X)^{YFP} subunits were coexpressed with human α1 and β2 subunits using different cDNA amounts (0.5 or 0.25 μg at a 1:1:1 cDNA ratio for each subunit). COS-7 cells were studied 2 d after transfection (Fig. 3*A*), and cultured hippocampal neurons were studied 8 d after transfection (Fig. 3*B*,*C*). Different amounts of cDNA were used to evaluate any artifact that might be attributable to subunit overexpression. When COS-7 cells were transfected with either 0.5 or 0.25 μg of each α1, β2, and γ2S^{YFP} subunit, wild-type γ2S^{YFP} subunits were distributed both intracellularly and on the cell surface (Fig. 3*A*, left). In contrast, in COS-7 cells transfected with either 0.5 or 0.25 μg of each α1, β2, and γ2S(Q351X)^{YFP} subunits, mutant γ2S(Q351X)^{YFP} subunits had no surface "ring-like" fluorescence signal, suggesting no surface expression, and were selectively retained in the ER as reported previously (Harkin et al., 2002; Kang et al., 2009b). When transfected with either 0.5 or 0.25 μg of each α1, β2, and γ2S(Q351X)^{YFP} subunit, the mutant subunits accumulated intracellularly. Total fluorescence intensities of mutant subunits were 1.78 ± 0.17-fold (0.5 μg) and 1.97 ± 0.22-fold (0.25 μg) higher than wild-type subunits (Fig. 3*D*).

In transfected neurons, γ2S^{YFP} subunits had a smooth distribution in both the soma and the dendrites (Fig. 3*B*,*C*, wt). In contrast, in neurons expressing mutant subunits, γ2S(Q351X)^{YFP} subunits were concentrated in the somata, and only minimal fluorescence signal was detected in axons and dendrites (Fig. 3*B*,*C*, mut). The ratios of fluorescence intensities in the somata over the processes were quantified, and the counts from neurons expressing wild-type γ2S^{YFP} subunits of each experiment were averaged and arbitrarily taken as 1. The counts from neurons expressing the mutant γ2S(Q351X)^{YFP} were normalized to the wild type. The normalized ratio of fluorescence in the somata over processes in neurons expressing the mutant subunits were higher than wild-type subunit (4.1 ± 0.09) (Fig. 3*E*), indicating that the fluorescence-tagged mutant subunits were accumulated in the somata with no or minimal expression in the axons and dendrites. In addition, neurons with higher expression of the mutant subunits often appeared to become less healthy and were associated with cell death in some transfected neurons (supplemental Fig. 2, available at www.jneurosci.org as supplemental material). However, it is unknown whether this neuronal death caused by the presence of the mutant protein occurs in patients and, if so, the time course of neuronal death. Study of neurons from mutation harboring knock-in mice would better reflect the course of the disease in humans. A thorough study focusing on the signaling pathways that engage the mutant protein metabolism and neuronal injury and death is needed. Nonetheless, accumulation of the nonfunctional mutant protein inside neurons is likely to cause neuronal dysfunction that may lead to cell dysfunction or death triggered by other forms of cellular stress or with time.

Mutant γ2S(Q351X) subunits were degraded slowly but formed SDS-resistant, high-molecular-mass protein complexes rapidly

Misfolded and truncated proteins are often degraded rapidly within cells so we performed [^{35}S]methionine radiolabeling pulse-chase experiments to determine whether mutant subunits had an altered rate of degradation. HEK 293T cells were transfected with either wild-type γ2^{FLAG} or mutant γ2S(Q351X)^{FLAG} subunits and incubated for 48 h. After radionuclide labeling for 20 min, cells were lysed after a 0, 1, 2, 4, or 6 h "chase" without (Fig. 4*A*,*B*) or with (supplemental Fig. 2, available at www.jneurosci.org as supplemental material) addition of cycloheximide (CHX) (100 μg/ml) to the chase medium to block protein synthesis. The amount of wild-type subunit protein (50 + 100 kDa) declined exponentially during the chase with a half-life of 115 min without CHX (Fig. 4*B*) or 100 min with CHX (supplemental Fig. 3, available at www.jneurosci.org as supplemental material). In contrast, the amount of mutant subunit

protein (40 + 80 kDa) initially increased and then, at 2 h of chase, declined to 94 or 96% of control radioactivity at time 0, with or without blockade of protein synthesis by CHX, and thus, the chase data points for the mutant subunit could not be fitted with a single-exponential function. However, the total amount of mutant subunit was greater than that of wild-type subunit at each chase time point with or without CHX (supplemental Fig. 3, available at www.jneurosci.org as supplemental material), indicating that the mutant γ2S(Q351X) subunit had a reduced rate of degradation. The higher-molecular-mass complex band of the mutant subunit was denser than the wild-type subunit band at each chase time with or without CHX (data not shown). Of note, the radionuclide counts of the mutant γ2S(Q351X) subunit was higher in the early chase time points (1 and 2 h) when there was no blockade of synthesis with CHX (Fig. 4*A*,*B*), but this increase was attenuated when protein synthesis was blocked with CHX (supplemental Fig. 3, available at www.jneurosci.org as supplemental material). This early increase of radioactivity has been seen commonly in our pulse-chase experiments when there is no blockade of protein synthesis (Gallagher et al., 2007) and is likely caused by accumulation of mutant subunits attributable to slow degradation and continuing synthesis.

To compare the rate of biosynthesis of wild-type γ2S and mutant γ2S(Q351X) subunits, we pulse-labeled cells transfected with $\gamma2S^{FLAG}$ or $\gamma2S(Q351X)^{FLAG}$ subunits with [^{35}S]methionine for 0, 5, 10, 15, and 20 min (Fig. 4*C*) and determined subunit levels at each time point. Normalized to the total wild-type (50 + 100 kDa) or mutant (40 + 80 kDa) subunit protein labeled for 20 min, there were no significant differences in the total amount of wild-type or mutant subunits (Fig. 4*D*) or the amount of high-molecular-mass complex for each labeling time point (data not shown) and, thus, no differences in their rates of biosynthesis. Although more prominent for mutant subunits, both wild-type and mutant subunits formed high-molecular-mass protein complexes within 5 min of translation, and the high-molecular-mass band became prominent within 10 min of labeling (Fig. 4*C*).

Wild-type γ2S subunits formed high-molecular-mass protein complexes when expressed alone or coexpressed in excess of partnering subunits

In addition to forming high-molecular-mass complexes when expressed alone, wild-type γ2S subunits also formed them when expressed in excess relative to α1 and β2 subunits. When α1 and β2 subunits were coexpressed with a reduced amount of γ2S subunits (cDNA ratio of 1:1:0.5), minimal high-molecular-mass complex was present (Fig. 5*A*). However, with coexpression of an excess of γ2S subunits (α1/β2/γ2S cDNA ratios of 1:1:2.5, 1:1:5, and 1:1:10), the high-molecular-mass complexes increased substantially (Fig. 5*A*,*B*). The ratio of the high-molecular-mass complex (100 kDa band) to the lower molecular band (50 kDa band) was only ~2% when expressed with a reduced amount of γ2S subunits (cDNA ratio of 1:1:0.5), but the ratio increased to ~16, 24, or 40% when expressed with an excess of γ2S subunits. In contrast, the γ2S(Q351X) subunit high molecular complexes or aggregates were substantial even at a ratio of 1:1:0.5 for α1/β2/γ2S(Q351X) subunit cDNAs, and the high molecular complex signals became saturated with higher cDNA ratios (Fig. 5*A*).

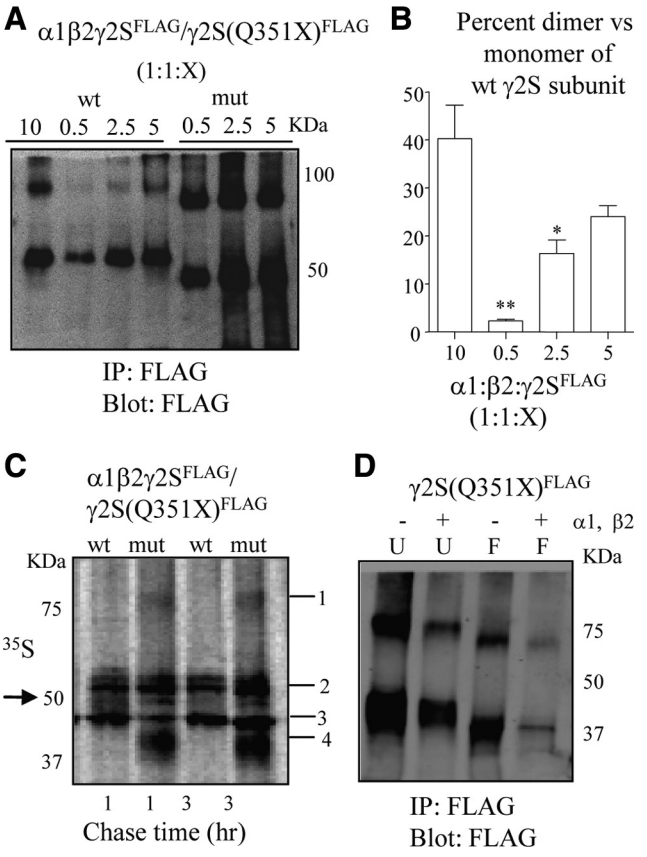

Figure 5. Wild-type γ2S subunits (wt) only formed high-molecular-mass protein complexes with coexpressed α1 and β2 subunits when they were in excess relative to α1 and β2 subunits, but mutant γ2S(Q351X) subunits (mut) formed high-molecular-mass protein complexes with or without coexpression of α1 and β2 subunits. ***A***, Cells were cotransfected with α1, β2, and $\gamma2S^{FLAG}$ subunits at different cDNA ratios (1:1:10, 1:1:0.5, 1:1:2.5, or 1:1:5). The total amount of cDNA was normalized to the empty vector pcDNA. The immunopurified subunits were analyzed by immunoblot that was probed with an anti-FLAG antibody. ***B***, The ratios of total IDVs of the higher molecular band (100 kDa) or the dimer band over the lower molecular band (50 kDa) or the monomer band in each condition were plotted (*$p < 0.05$, **$p < 0.01$ vs 1:1:10; $n = 4$). ***C***, Cells coexpressing α1 and β2 subunits with wild-type γ2S and mutant $\gamma2S(Q351X)^{FLAG}$ subunits (cDNA ratio of 1:1:1) were pulse chased for 1 or 3 h and lysed for immunopurification and SDS-PAGE. Band 1 indicates the high-molecular-mass protein complex, and band 4 indicates $\gamma2S(Q351X)^{FLAG}$ subunit monomers. There were multiple bands in the band 2 area that indicate the wild-type $\gamma2S^{FLAG}$ and coimmunoprecipitated α1 and β2 subunits. Band 3 indicates a nonspecific band. The arrow points to the $\gamma2S^{FLAG}$ subunit band. ***D***, Cells expressing mutant $\gamma2S(Q351X)^{FLAG}$ subunits alone (3 μg of cDNA) or coexpressed with α1 and β2 subunits (1 μg of cDNA each) were lysed for immunopurification, treated (F) or untreated (U) with PNGase F, and fractionated by SDS-PAGE (***C*** and ***D*** were representative gels of four experiments).

Mutant γ2S(Q351X) subunits were more prone than wild-type subunits to form high-molecular-mass protein complexes with or without coexpression of partnering subunits

When $\alpha1\beta2\gamma2S^{FLAG}$ or $\alpha1\beta2\gamma2S(Q351X)^{FLAG}$ subunits were coexpressed in HEK 293T cells at an equal subunit cDNA ratio of 1:1:1, and the cells were pulse labeled with [^{35}S]methionine for 20 min followed by a 1 or 3 h chase (Fig. 5*C*) (supplemental Fig. 4*A*, available at www.jneurosci.org as supplemental material), high-molecular-mass protein complexes were not detectable with wild-type subunit expression but were detected with mutant subunit expression at both 1 and 3 h (Fig. 5*C*, band 1), with substantial amounts of mutant subunit monomers detected at each time point (Fig. 5*C*, band 4). Wild-type $\gamma2S^{FLAG}$ subunits could not be detected unambiguously because of the presence of mature and immature α1 and β2 subunits that had molecular masses similar to $\gamma2S^{FLAG}$ subunits (Fig. 5*C*, band 2).

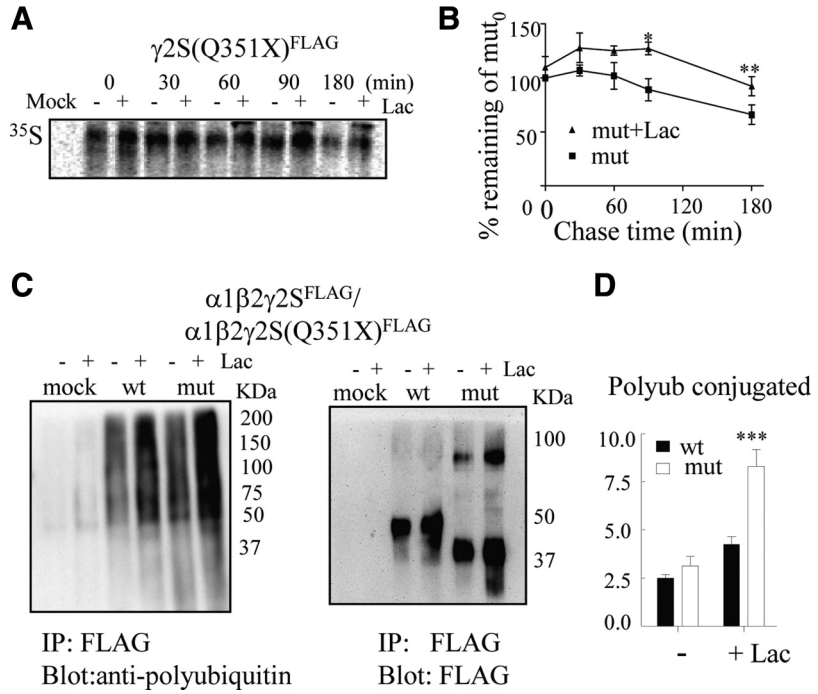

Figure 6. Mutant γ2S(Q351X) subunits were degraded through the ubiquitin–proteasome pathway. ***A***, Cells mock transfected (mock) or transfected with γ2S(Q351X)^{FLAG} subunits were labeled with [^{35}S]methionine for 20 min, followed by chase in the absence (−) or presence (+) of the proteasome inhibitor lactacystin (Lac, 10 μM) for the indicated time periods. ***B***, The percentage radioactivity relative to the amount of radioactivity measured at time 0 for mutant subunits without lactacystin treatment in the absence (−) or presence (+) of lactacystin was plotted at each chase time (*$p < 0.05$, **$p < 0.01$ vs mutant without lactacystin; $n = 4$). ***C***, Cells were mock transfected or transfected with γ2S^{FLAG} (wt) or γ2S^{FLAG}(Q351X) (mut) subunits and were incubated for 4 h in the absence or presence of 10 μM lactacystin before cell lysis. The immunopurified subunits were analyzed by immunoblot probed with an antibody against polyubiquitin (left) or FLAG (right) ($n = 9$). ***D***, The total IDVs of polyubiquitin were measured from ~37 to 200 kDa in both the wild-type and the mutant subunits. The normalized amounts of polyubiquitin IDVs from pooled data were plotted ($n = 9$; ***$p < 0.001$ vs wild type + lactacystin).

The high-molecular-mass protein complexes detected on SDS-PAGE with expression of γ2S(Q351X)^{FLAG} subunits alone or with partnering α1 and β2 subunits contained γ2S(Q351X)^{FLAG} subunits and had similar molecular masses

Mutant γ2S(Q351X)^{FLAG} subunits were immunopurified from lysates of cells transfected with γ2S(Q351X)^{FLAG} subunits without (supplemental Fig. 4*B*, available at www.jneurosci.org as supplemental material) (Fig. 5*D*, −) or with (Fig. 5*D*, +) α1 and β2 subunits. The mutant subunits then were treated (Fig. 5*D*; F) or not treated (Fig. 5*D*; U) with PNGase F to remove attached *N*-glycans and immunoblotted with anti-FLAG antibody. The protein complexes obtained with expression of γ2S(Q351X)^{FLAG} subunits with or without α1 and β2 subunits migrated at the same molecular mass before PNGase F treatment (Fig. 5*D*; U) and were shifted to the same lower molecular mass after PNGase F treatment (Fig. 5*D*; F). The protein complex molecular mass was approximately twice that of the predicted mass of mutant subunits, suggesting that the high-molecular-mass protein complexes present on SDS-PAGE were likely modified γ2S(Q351X) subunit dimers. In addition, a protein complex with a molecular mass that was larger than the "potential dimer" was occasionally detected and migrated between 150 and 250 kDa, thus potentially being modified "multimers" composed of three or more mutant γ2S(Q351X) subunits. In conclusion, the core structure of the γ2S(Q351X) subunit high-molecular-mass protein complexes observed in SDS gel either when γ2S(Q351X) subunits were expressed alone or with α1 and β2 subunits contained mutant γ2S(Q351X) subunits that were likely mutant subunit dimers.

Proteasome inhibition increased levels of the high-molecular-mass protein complexes and both wild-type γ2S and mutant γ2S(Q351X) subunit monomers

Other mutant $GABA_A$ receptor subunits associated with genetic epilepsy syndromes are degraded through the ubiquitin–proteasome pathway (Gallagher et al., 2007; Kang et al., 2009a), and thus we determined whether γ2S(Q351X) subunits were degraded by this pathway. We first used [^{35}S]methionine pulse chase to determine the degradation rate of mutant γ2S(Q351X) subunits in the presence or absence of proteasomal inhibition by lactacystin (10 μM). After [^{35}S]methionine pulse labeling, the transfected HEK 293T cells were switched to the chase medium with or without lactacystin for a 0, 30, 60, 90, or 180 min chase (Fig. 6*A*). When normalized to the total γ2S(Q351X) subunit protein level at time 0 without lactacystin treatment, mutant subunit protein levels were increased 125–140% with lactacystin treatment at all chase times >60 min (Fig. 6*B*).

Mutant subunits were conjugated with more ubiquitin than wild-type subunits

Because mutant proteins should be polyubiquitinated before degradation by the ubiquitin–proteasome pathway, we determined whether mutant γ2S(Q351X) subunits were polyubiquitinated. HEK 293T cells were transfected with both wild-type γ2S^{FLAG} and mutant γ2S(Q351X)^{FLAG} subunits and incubated for 4 h with or without lactacystin (10 μM). The subunits were immunopurified using anti-FLAG antibody and analyzed by immunoblot probed with an antibody against polyubiquitin (Fig. 6*C*, left) or FLAG (Fig. 6*C*, right). The total IDVs of polyubiquitin were measured from ~37 to 200 kDa in both the wild-type and the mutant subunits. Proteasome inhibition increased polyubiquitination of both wild-type and mutant subunits (4.23 ± 0.42 vs 8.3 ± 0.89, $p = 0.0008$) (Fig. 6*C*), but mutant subunits were conjugated with more polyubiquitin than wild-type subunits (Fig. 6D). However, it is unknown whether the high-molecular-mass protein complex would conjugate more ubiquitin than the monomers or how much ubiquitin were conjugated by the high-molecular-mass protein complex.

Mutant γ2S(Q351X) subunits were degraded also through the lysosome pathway

Because lysosomal degradation is another major pathway for protein disposal, we compared mutant subunit protein degradation with and without lysosomal inhibition. HEK 293T cells were transfected with mutant γ2S(Q351X) subunits alone for 48 h. Immediately after [^{35}S]methionine labeling for 20 min, cells were switched to medium with or without the lysosome inhibitor chloroquine (100 μM) and incubated for 0, 30, 60, 90, and 180 min (Fig. 7*A*). Chloroquine is known to inhibit lysosomal hydrolases by reducing the acidification of the endosomal/lysosomal compartments. Bands from chloroquine-treated samples were more

intense within 30 min of treatment (137–189%). When normalized to the amount of total mutant protein at 0 min, there were significant increases in the amount of mutant subunit protein at all time points from 30 to 180 min with chloroquine treatment (Fig. 7*B*). With lysosome inhibition, we then compared the steady-state protein levels of both γ2S and γ2S(Q351X) subunits when coexpressed with α1 and β2 subunits (Fig. 7*C*). Incubation with chloroquine increased the total level of mutant, but not wild-type, subunits. Lysosome inhibition with chloroquine increased total mutant subunit levels (1.89 ± 0.20) (including subunit monomers and possibly dimers and tetramers) to a greater extent than total wild-type subunit levels (1.22 ± 0.23, $p = 0.03$) (Fig. 7*D*).

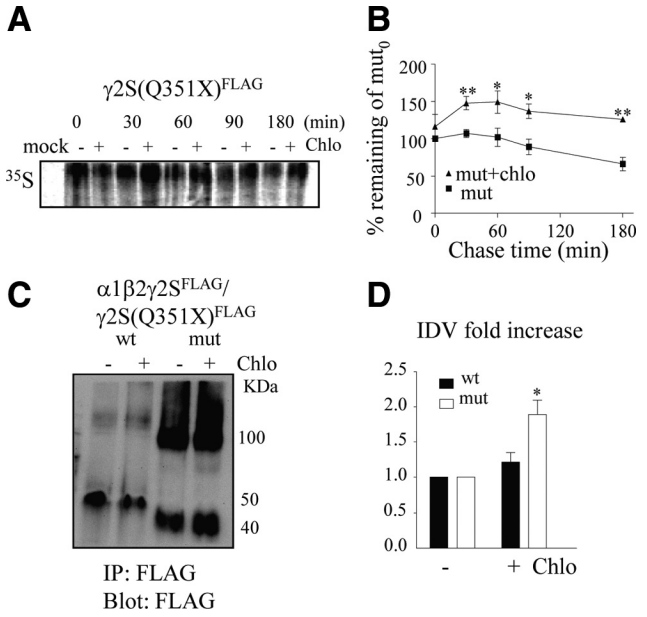

Figure 7. Mutant γ2S(Q351X) subunits were degraded through the lysosome pathway. ***A***, Cells mock transfected (mock) or transfected with γ2S(Q351X)^{FLAG} subunits were labeled with [^{35}S]methionine for 20 min, followed by chase in the absence (−) or presence (+) of chloroquine (Chlo, 100 μM) for the indicated time periods. The cells were lysed, immunopurified using anti-Flag antibody, and analyzed by SDS-PAGE. ***B***, The percentage radioactivity relative to the amount of radioactivity measured at time 0 for mutant subunits without chloroquine treatment in the absence (−) or presence (+) of chloroquine was plotted (*$p < 0.05$, **$p < 0.01$ vs mutant without chloroquine; $n = 4$). ***C***, HEK 293T cells expressing equimolar concentrations of wild-type (wt) and mutant (mut) α1β2γ2S^{FLAG} subunits were incubated without (−) or with (+) chloroquine (100 μM) for 4 h. The total lysates were immunopurified and immunoblotted with rabbit polyclonal anti-FLAG antibody. ***D***, The total γ2 subunit protein IDVs with chloroquine treatment were normalized to the untreated group (*$p < 0.05$ vs wild type + chloroquine; $n = 4$).

Formation of SDS-resistant, high-molecular-mass protein complexes is a common phenomenon for truncated and misfolded mutant $GABA_A$ receptor subunit proteins

Although most epilepsy mutations are associated with a single family and the γ2 subunit mutation Q351X is associated with a small pedigree, approximately one-third of human genetic diseases, including epilepsy, are caused by nonsense mutations or other types of mutations that generate PTCs. We determined whether other $GABA_A$ receptor subunit nonsense mutations that cause subunit truncation would also result in the formation of high-molecular-mass protein complexes. We generated a series of γ2 subunit nonsense mutations that were N terminal to the Q351X mutation, including G234X at the C-terminal end of the N terminus, N258X at the end of TM1, R284X at the C-terminal end of TM2, and V321X at the C-terminal end of TM3 (Fig. 8*A*). Similar to γ2S(Q351X) mutant subunits, all of these nonsense mutations generated truncated subunits that formed high-molecular-mass protein complexes (Fig. 8*B*), although the ratio of the amount of high-molecular-mass protein complexes to the amount of subunit monomers varied. When normalized to the dimers (Fig. 8*B*, red arrows) over monomers (Fig. 8*B*, green arrows) of the wild-type subunits, all of the truncated mutant γ2S subunits had increased dimer to monomer ratios (each mutant subunit ratio was divided by the wild-type subunit ratio), ranging from an increase of ~2-fold to 2.5-fold, indicating that mutant subunits were more prone to form dimers ($n = 6$). However, our data might not be an accurate estimation of the exact ratio of multimers over monomers because the formation of dimers and monomers may be very dynamic, and we did not include tetramer or even high-molecular-mass protein complexes.

We also generated mutations that would impair protein folding by deleting a major portion of the TM3–TM4 loop in α1, β2, and γ2 subunits (Fig. 8*D*). Disruption of the TM3–TM4 loops of β2 and γ2S, but not of α1, subunits produced substantial high-molecular-mass protein complexes on SDS-PAGE (Fig. 8*E*, Loop del), but the amount of the protein complexes was greater for γ2S (74.1%) than β2 (29.2%, $p = 0.0015$ vs γ2S loop del) loop deleted subunits. In addition, mutant γ2S(Q351X) subunits produced more high-molecular-mass protein complexes than γ2S loop deleted subunits (153.5%, $p = 0.0035$ vs γ2S Loop del, $n = 4$) (Fig. 8*F*). These data suggest that formation of SDS-resistant, high-molecular-mass protein complexes is a common phenomenon with truncated and misfolded $GABA_A$ receptor subunit proteins and that some mutant or misfolded subunits are more prone to form aggregates than others. The cellular and functional consequences of these truncations, however, could differ depending on their properties such as ability to oligomerize with other subunits, their stability, and the likelihood of each mutant subunit to self-associate.

Disruption of the N-terminal disulfide bond destabilized the mutant protein, suggesting that γ2 subunit cysteines C151 and C165 in the signature Cys loop were likely involved in formation of subunit complexes

What is the basis for the mutant γ2(Q351X) subunits to form complexes? It has been reported that disulfide bonds stabilize proteins and accelerate folding (Matsumura et al., 1989; Fei and Perrett, 2009). Thus, we mutated the γ2 subunit cysteines C151 and C165 in the signature Cys loop to alanine to determine whether they were important for formation of the high-molecular-mass protein complexes (Fig. 8*G*). Transfection of HEK 293T cells with FLAG-tagged γ2(Q351X)^{FLAG} subunits resulted in formation of substantial high-molecular-mass complexes (Fig. 8*H*, con). Mutation of C151, C165, or both cysteines substantially reduced formation of the higher-molecular-mass protein complexes and facilitated protein degradation (Fig. 8*H*). The same phenomenon of destabilizing the protein by disrupting the disulfide bond was observed with wild-type subunits but to a lesser extent (supplemental Fig. 5, available at www.jneurosci.org as supplemental material). When normalized to mutant γ2(Q351X)

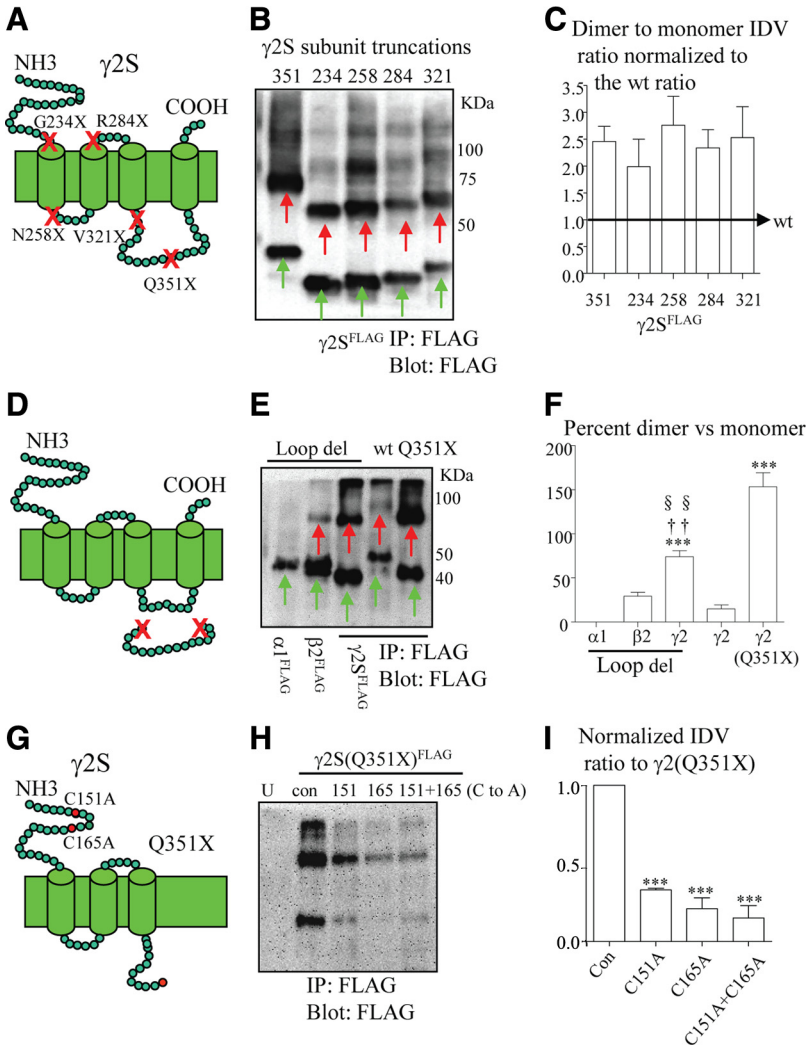

Figure 8. Multiple truncated or misfolded $GABA_A$ receptor subunits formed SDS-resistant protein complexes, and cysteines 151 and 165 in the N terminus were involved in the formation of the SDS-resistant protein complexes. ***A***, Schematic locations of mutations that were introduced to produce truncated γ2S subunits were indicated by red crosses. ***B***, Total lysates of HEK 293T cells transfected with γ2S(Q351X)^{FLAG}, γ2S(G234X)^{FLAG}, γ2S(N258X)^{FLAG}, γ2S(R284X)^{FLAG}, and γ2S(V321X)^{FLAG} subunits were immunopurified using anti-FLAG antibody and analyzed by SDS-PAGE. ***C***, The ratios of the total IDVs of dimers over monomers for each truncated γ2S subunit in ***B*** were plotted. The data were normalized to wild-type γ2S^{FLAG} subunit (wt). The ratio of the total IDVs of dimer in wild type was arbitrarily taken as 1 ($n = 6$) (***C***). ***D***, Schematic topology of α1, β2, and γ2S subunits with deletions of a major portion of the intracellular TM3–TM4 loops were marked with red crosses to represent the portion of the intracellular TM3–TM4 loop that was removed. ***E***, Total lysates of HEK 293T cells transfected with α1^{FLAG}, β2^{FLAG}, and γ2S^{FLAG} with loop deletion, γ2S^{FLAG}(wt) and γ2S(Q351X)^{FLAG} subunits, and their partnering subunits were immunopurified using anti-FLAG antibody and analyzed by SDS-PAGE. The loop-deleted α1^{FLAG} subunits were cotransfected with wild-type β2 and γ2S subunits; the loop-deleted β2^{FLAG} subunits were cotransfected with α1 and γ2S subunits; and the wild-type, loop-deleted and mutant γ2S subunits were cotransfected with α1 and β2 subunits. ***F***, The percentages of total IDVs of dimers over monomers for each condition were plotted [$n = 4$; ***$p < 0.001$ vs wild type; $^{\dagger\dagger}p < 0.01$ vs γ2S(Q351X)^{FLAG}; $^{\S\S}p < 0.01$ vs β2^{FLAG} loop deletion]. In ***B*** and ***E***, the green arrows designated mutant γ2S^{FLAG} subunits that migrated as monomers, and the red arrows designated potential subunit dimers. ***G***, Schematic topology of γ2S(Q351X) subunits with cysteines C151 and C165 in the signature Cys-loop mutated to alanines. ***H***, Total lysates of HEK 293T cells untransfected (U) or transfected with γ2S(Q351X)^{FLAG} subunits without cysteines mutated (con) or with mutant γ2S(Q351X)^{FLAG} subunits containing mutations in C151 (151), C165 (165), or both (151 + 165). Mutant γ2S(Q351X)^{FLAG} subunits without or with mutation of the cysteines were immunopurified using anti-FLAG antibody and analyzed by SDS-PAGE. ***I***, The total IDVs in ***H*** for γ2S(Q351X)^{FLAG} subunits without or with mutation of the cysteines were plotted. The data were normalized to the γ2S(Q351X)^{FLAG} subunit without mutant cysteines. The total IDV of γ2S(Q351X)^{FLAG} subunits was arbitrarily taken as 1 [$n = 4$ from four different transfections; ***$p < 0.001$ vs γ2S(Q351X)^{FLAG} subunit].

subunits without interruption of the cysteine loop, mutation of either cysteine reduced the total amount of both high-molecular-mass protein complex and subunit monomer mutant subunit protein to less than one-third (0.33 ± 0.01 for C151A, 0.21 ± 0.07 for C165A, and 0.15 ± 0.08 for C151A + C165A) (Fig. 8*I*). However, protein aggregation is a very complex process and usually involves multiple protein domains. It is not know whether other regions of the subunit are also involved in the dimerization or aggregation of this mutant protein.

Discussion

The GABRG2(Q351X) mutation may cause more than impaired receptor trafficking

Although the majority of children with $GABA_A$ receptor or sodium channel gene mutations only have mild epilepsy phenotypes, there is a small subgroup of children harboring these mutations that manifest the more severe disease phenotype Dravet syndrome, which includes refractory seizures, a progressive disease course, impaired development, and cognitive decline. Genetic studies have linked this subgroup to truncation mutations frequently to SCN1A and occasionally to GABRG2 genes (Scheffer et al., 2001; Berkovic et al., 2006; Hirose, 2006). The underlying bases for the association of these truncation mutations with the more severe epilepsy phenotype are not clear and may be partially attributable to the complete loss of function of the mutant allele in contrast to missense mutations that generally have only impaired function of the mutant allele. Our previous work demonstrated that one of these mutations, GABRG2(Q351X) associated with GEFS+, including Dravet syndrome, had more impaired α1β2γ2S $GABA_A$ receptor channel function than could be explained by the loss of one allele (Crestani et al., 1999). Thus, the GABRG2(Q351X) mutation may reduce α1β2γ2S receptor channel function more than either the heterozygous GABRG2 gene knock-out (Crestani et al., 1999) or the heterozygous GABRG2(R43Q) epilepsy mutation (Tan et al., 2007). In addition to the loss of inhibition produced by the GABRG2 (Q351X) mutation, we observed an SDS-resistant, high-molecular-mass protein complex that contained γ2S(Q351X) subunits. However, the cellular consequence of the presence of the high-molecular-mass protein complex is not clear. Although our data demonstrated that the protein aggregation and formation of high-molecular-protein complex was a common phenomenon for γ2S^{FLAG} subunits, other truncated $GABA_A$ receptor subunits, such as the mutant α1(S326fs328X) subunit associated with childhood absence epilepsy, were unstable, were degraded rapidly (Kang et al., 2009a), and did not form stable high-molecular-mass protein complexes. Furthermore, some truncation mutations may trigger nonsense-mediated mRNA decay, thus eliminating the majority of the

mutant protein and causing haploinsufficiency for the subunit. Therefore, despite the frequent genetic association of patients with Dravet syndrome with nonsense mutations of SCN1A and GABRG2, it is still unknown whether and how a truncated SCN1A or GABRG2 subunit worsens a disease phenotype by mechanisms in addition to a reduced channel function.

Formation of SDS-resistant, high-molecular-mass protein complexes is a feature of several neurodegenerative diseases

The presence of the SDS-resistant high-molecular-mass protein complexes was surprising because formation of protein complexes or protein aggregates is a hallmark of many neurodegenerative diseases (Tran and Miller, 1999; Wanker, 2000; Rajan and Kopito, 2005) but in general not of genetic epilepsy syndromes. Formation of SDS-resistant, high-molecular-mass protein complexes or insoluble protein aggregates is a feature of many neurodegenerative diseases, including Parkinson's disease and Huntington's disease. Many of the mutations that cause dominantly inherited neurodegenerative disease have been demonstrated to increase dramatically the propensity of the mutant gene product to self-associate into protein aggregates both *in vitro* and *in vivo* (Fink, 1998). This supports the widely accepted hypothesis that this feature of protein aggregation underlies the molecular pathogenesis of many neurodegenerative diseases. The presence of misfolded or aggregated mutant proteins has been demonstrated to activate the unfolded protein response, leading to upregulation of molecular chaperones. Additional study focusing on the signaling pathways of the unfolded protein response and activities of molecular chaperones in the cells harboring the mutant γ2(Q351X) subunits will help determine whether the mutant subunit has cellular consequences common to other trafficking-defective proteins.

Mutant γ2S(Q351X) subunits adopt a relatively stable conformation rapidly after translation and have a slower degradation rate than wild-type γ2S subunits

What is the basis for mutant γ2S(Q351X) subunit protein accumulation and aggregation? Our data demonstrated that both wild-type γ2S and mutant γ2S(Q351X) subunits formed high-molecular-mass protein complexes within 5–10 min of the onset of translation. Occasionally with pulse labeling at time 0, whenever the monomer was detected, the high-molecular-mass protein complexes were present, suggesting that formation of the aggregates was spontaneous. However, in our experiments, subunit radioactivity was not detected reliably until 5 min after pulse labeling. Thus, we concluded that aggregate formation was likely cotranslational in the ER. Formation of the protein complexes with expression of wild-type γ2S subunits, however, occurred significantly only in the absence of α1 and β2 subunits, suggesting that oligomerization with partnering subunits masked the γ2S subunit domain for self-association or inhibited misfolding and aggregation of wild-type γ2S subunits.

In contrast, mutant γ2S(Q351X) subunits formed high-molecular-mass protein complexes regardless of the presence of other wild-type subunits and accumulated attributable to slowed degradation. A similar accumulation of mutant protein has been observed for mutant α-Synuclein(A53T), which is associated with Parkinson's disease (Bennett et al., 1999), and the degradation rate of α-Synuclein(A53T) protein was 50% slower than that of the wild-type protein. Our pulse-chase experiments demonstrated that, when expressed alone, mutant subunits were more stable than wild-type subunits. However, under more physiological conditions with coexpression of wild-type γ2S and partnering α and β subunits, wild-type γ2S subunits would be subject to more complicated posttranslational modifications and recycling and would traffic to the cell surface and to synapses. Thus, the half-life of wild-type γ2S subunits should not be the same as that observed in heterologous expression systems *in vitro*, but it is likely that mutant subunits adopt a stable conformation and degrade slowly both *in vitro* and *in vivo*.

The high-molecular-mass protein complex may be composed of modified dimeric γ2S mutant subunits that form a core structure for a larger protein complex

We propose that the high-molecular-mass protein complex observed on SDS-PAGE was likely composed of modified dimers of γ2S(Q351X) subunits. The increase in molecular mass of the protein complexes for both wild-type γ2S and mutant γ2S(Q351X) subunits correlated with a difference in molecular mass of their monomers. A similar molecular mass shift was observed with expression of other γ2S subunit nonsense mutations and γ2S subunits with deletion of the intracellular TM3–TM4 loop, again suggesting formation of subunit dimers and that the deletion of the TM3–TM4 loop structure or exposure of hydrophobic residues attributable to protein misfolding caused subunit self-association. The band detected in neurons that migrated at ~160 kDa was a potential tetramer formed by association of dimers with longer incubation time, which thus became more prominent with the longer time between transfection and harvesting of neurons (8 d) than of HEK 293T cells (2 d). Mutant protein dimers have been observed also with mutant Rhodopsin (P23H) associated with autosomal-dominant retinitis pigmentosa (Rajan and Kopito, 2005). It is unknown, however, whether or not the subunit monomer or the dimeric subunit protein complex is cytotoxic and, if so, which is more toxic. In addition, our observation was made on SDS-PAGE, and the detergent used may have caused dissociation of additional, more loosely conjugated proteins, leaving only the most tightly conjugated, protein core structure. Under physiological conditions, multiple wild-type partnering subunits coexist in a crowded cellular environment, and it is possible that the aggregates may contain also those partnering subunits such as α1 and β2 subunits depending on their relative binding affinities and on the relative abundance of each subunit. Nevertheless, the presence of the higher-molecular-mass protein complex on SDS-PAGE suggests that the proteins associated with mutant γ2 subunits are bound very tightly and with high stability.

Formation of SDS-resistant, high-molecular-mass protein complexes is a common phenomenon for truncated or misfolded $GABA_A$ receptor subunit proteins and disruption of the signature Cys loop destabilized the mutant subunit protein

The proband carrying the GABRG2(Q351X) mutation presented with a severe type of epilepsy, Dravet syndrome. In addition to the GABRG2(Q351X) mutation, the GABRG2(Q1X) nonsense mutation has also been associated with twin sisters with Dravet syndrome in a small Japanese pedigree (Hirose, 2006). It is likely that these nonsense mutations result in either truncated or nonfunctional proteins with relatively stable conformations or in exposure of hydrophobic residues that causes rapid self-association to form aggregates. Although mutant protein aggregation may be a complex process and multiple domains or segments in the protein may be involved, the γ2 subunit cysteines C151 and C165 at least contribute to the mutant protein dimerization and aggregation. The presence of the stable trafficking-deficient mutant pro-

tein may be toxic to cells over a lifelong disease course, in addition to its loss of biological function and/or to its destructive interaction with wild-type partnering subunits (Mezghrani et al., 2008; Kang and Macdonald, 2009), thus resulting a more severe disease phenotype compared with simple gene deletion knock-out condition. This study suggests that an ion channel mutation such as GABRG2(Q351X) associated with a genetic epilepsy, Dravet syndrome, may have additional pathological actions in addition to simple loss of neuronal inhibition or GABAergic signaling in early stages of brain development. This extra pathological action caused by inefficient subunit protein degradation and subunit aggregation may disturb intracellular signaling pathways, alter expression of genes that are critical for neurodevelopment, and lead to neuronal dysfunction, rendering neurons more vulnerable to cellular stresses over time. However, it is unclear whether the presence of the mutant protein complex would worsen the disease phenotype *in vivo*. Future work comparing GABRG2 (Q351X) knock-in mice with gene deletion GABRG2 knock-out mice and/or with knock-in mice, such as GABRG2(R43Q) knock-in mice, that have a mutation that does not result in formation of stable aggregates may further elucidate the pathological effect of the presence of the mutant aggregates.

References

Baulac S, Huberfeld G, Gourfinkel-An I, Mitropoulou G, Beranger A, Prud'homme JF, Baulac M, Brice A, Bruzzone R, LeGuern E (2001) First genetic evidence of $GABA_A$ receptor dysfunction in epilepsy: a mutation in the gamma2-subunit gene. Nat Genet 28:46–48.

Bennett MC, Bishop JF, Leng Y, Chock PB, Chase TN, Mouradian MM (1999) Degradation of alpha-synuclein by proteasome. J Biol Chem 274:33855–33858.

Berke SJ, Paulson HL (2003) Protein aggregation and the ubiquitin proteasome pathway: gaining the UPPer hand on neurodegeneration. Curr Opin Genet Dev 13:253–261.

Berkovic SF, Harkin L, McMahon JM, Pelekanos JT, Zuberi SM, Wirrell EC, Gill DS, Iona X, Mulley JC, Scheffer IE (2006) De-novo mutations of the sodium channel gene SCN1A in alleged vaccine encephalopathy: a retrospective study. Lancet Neurol 5:488–492.

Cohen-Gadol AA, Bradley CC, Williamson A, Kim JH, Westerveld M, Duckrow RB, Spencer DD (2005) Normal magnetic resonance imaging and medial temporal lobe epilepsy: the clinical syndrome of paradoxical temporal lobe epilepsy. J Neurosurg 102:902–909.

Crestani F, Lorez M, Baer K, Essrich C, Benke D, Laurent JP, Belzung C, Fritschy JM, Lüscher B, Mohler H (1999) Decreased GABAA-receptor clustering results in enhanced anxiety and a bias for threat cues. Nat Neurosci 2:833–839.

Fei L, Perrett S (2009) Disulfide bond formation significantly accelerates the assembly of Ure2p fibrils because of the proximity of a potential amyloid stretch. J Biol Chem 284:11134–11141.

Fink AL (1998) Protein aggregation: folding aggregates, inclusion bodies and amyloid. Fold Des 3:R9–R23.

Gallagher MJ, Ding L, Maheshwari A, Macdonald RL (2007) The GABAA receptor alpha1 subunit epilepsy mutation A322D inhibits transmembrane helix formation and causes proteasomal degradation. Proc Natl Acad Sci U S A 104:12999–13004.

Harkin LA, Bowser DN, Dibbens LM, Singh R, Phillips F, Wallace RH, Richards MC, Williams DA, Mulley JC, Berkovic SF, Scheffer IE, Petrou S (2002) Truncation of the $GABA_A$-receptor gamma2 subunit in a family with generalized epilepsy with febrile seizures plus. Am J Hum Genet 70:530–536.

Hirose S (2006) A new paradigm of channelopathy in epilepsy syndromes: intracellular trafficking abnormality of channel molecules. Epilepsy Res 70 [Suppl 1]:S206–S217.

Kamiya K, Kaneda M, Sugawara T, Mazaki E, Okamura N, Montal M, Makita N, Tanaka M, Fukushima K, Fujiwara T, Inoue Y, Yamakawa K (2004) A nonsense mutation of the sodium channel gene SCN2A in a patient with intractable epilepsy and mental decline. J Neurosci 24:2690–2698.

Kang JQ, Macdonald RL (2004) The $GABA_A$ receptor $\gamma 2$ subunit R43Q mutation linked to childhood absence epilepsy and febrile seizures causes retention of $\alpha 1\beta 2\gamma 2S$ receptors in the endoplasmic reticulum. J Neurosci [Erratum (2004) 24:1p following 9126; Kang Jingqiong (corrected to Kang, Jing-Qiong)] 24:8672–8677.

Kang JQ, Macdonald RL (2009) Making sense of nonsense $GABA_A$ receptor mutations associated with genetic epilepsies. Trends Mol Med 15:430–438.

Kang JQ, Shen W, Macdonald RL (2009a) Two molecular pathways (NMD and ERAD) contribute to a genetic epilepsy associated with the $GABA_A$ receptor GABRA1 PTC mutation, 975delC, S326fs328X. J Neurosci 29:2833–2844.

Kang JQ, Shen W, Macdonald RL (2009b) The GABRG2 mutation, Q351X, associated with generalized epilepsy with febrile seizures plus, has both loss of function and dominant-negative suppression. J Neurosci 29: 2845–2856.

Li SH, Lam S, Cheng AL, Li XJ (2000) Intranuclear huntingtin increases the expression of caspase-1 and induces apoptosis. Hum Mol Genet 9:2859–2867.

Linde L, Boelz S, Neu-Yilik G, Kulozik AE, Kerem B (2007) The efficiency of nonsense-mediated mRNA decay is an inherent character and varies among different cells. Eur J Hum Genet 15:1156–1162.

Lo WY, Botzolakis EJ, Tang X, Macdonald RL (2008) A conserved Cys-loop receptor aspartate residue in the M3–M4 cytoplasmic loop is required for $GABA_A$ receptor assembly. J Biol Chem 283:29740–29752.

Matsumura M, Signor G, Matthews BW (1989) Substantial increase of protein stability by multiple disulphide bonds. Nature 342:291–293.

Mezghrani A, Monteil A, Watschinger K, Sinnegger-Brauns MJ, Barrère C, Bourinet E, Nargeot J, Striessnig J, Lory P (2008) A destructive interaction mechanism accounts for dominant-negative effects of misfolded mutants of voltage-gated calcium channels. J Neurosci 28:4501–4511.

Ohmori I, Kahlig KM, Rhodes TH, Wang DW, George AL Jr (2006) Nonfunctional SCN1A is common in severe myoclonic epilepsy of infancy. Epilepsia 47:1636–1642.

Rajan RS, Kopito RR (2005b) Suppression of wild-type rhodopsin maturation by mutants linked to autosomal dominant retinitis pigmentosa. J Biol Chem 280:1284–1291.

Scheffer IE, Berkovic SF (1997) Generalized epilepsy with febrile seizure plus. a genetic disorder with heterogeneous clinical phenotypes. Brain 120:479–490.

Scheffer IE, Wallace R, Mulley JC, Berkovic SF (2001) Clinical and molecular genetics of myoclonic-astatic epilepsy and severe myoclonic epilepsy in infancy (Dravet syndrome). Brain Dev 23:732–735.

Shi X, Yasumoto S, Nakagawa E, Fukasawa T, Uchiya S, Hirose S (2009) Missense mutation of the sodium channel gene SCN2A causes Dravet syndrome. Brain Dev 31:758–762.

Tan HO, Reid CA, Single FN, Davies PJ, Chiu C, Murphy S, Clarke AL, Dibbens L, Krestel H, Mulley JC, Jones MV, Seeburg PH, Sakmann B, Berkovic SF, Sprengel R, Petrou S (2007) Reduced cortical inhibition in a mouse model of familial childhood absence epilepsy. Proc Natl Acad Sci U S A 104:17536–17541.

Tran PB, Miller RJ (1999) Aggregates in neurodegenerative disease: crowds and power? Trends Neurosci 22:194–197.

Wallace RH, Marini C, Petrou S, Harkin LA, Bowser DN, Panchal RG, Williams DA, Sutherland GR, Mulley JC, Scheffer IE, Berkovic SF (2001) Mutant $GABA_A$ receptor gamma2-subunit in childhood absence epilepsy and febrile seizures. Nat Genet 28:49–52.

Wanker EE (2000) Protein aggregation and pathogenesis of Huntington's disease: mechanisms and correlations. Biol Chem 381:937–942.

Xu S, Pang Q, Liu Y, Shang W, Zhai G, Ge M (2007) Neuronal apoptosis in the resected sclerotic hippocampus in patients with mesial temporal lobe epilepsy. J Clin Neurosci 14:835–840.